ADAPTIVE ENERGY-SENSITIVE X-RAY TECHNOLOGY FOR LONG-PULSE OPERATION OF MAGNETICALLY CONFINED THERMAL AND NON-THERMAL PLASMAS

[1]L. F. DELGADO-APARICIO, T. BARBUI, M. ONO, B. STRATTON, K. HILL, M. BITTER, N. PABLANT, J. WISNIEWSKI, R. ELLIS, [2]T. FONGHETTI, S. MAZZI, J. MORALES, P. MANAS, Y. SAVOYE-PEYSSON, X. LITAUDON, N. FEDORCZAK, R. DUMONT, P. MOREAU, F. IMBEAUX, A. EKEDAHL, B. CANTONE, J. C. HATCHRESSIAN, C. DECHELLE, P. MALARD, [3]J. WALLACE, [4]D. VEZINET AND [5]O. CHELLAI

[1]Princeton Plasma Physics Laboratory, Princeton, NJ, USA
[2]CEA, IRFM, Saint-Paul-les-Durance Cedex, France
[3]University of Wisconsin - Madison, Madison, Madison, WI, USA
[4]Commonwealth Fusion Systems, Devens, MA, USA
[5]Swiss Plasma Center, Ecole Polytechnique Federale de Lausanne, Lausanne, Switzerland

Email: ldelgado@pppl.gov

1. ABSTRACT

Novel multi-energy soft and hard x-ray (ME-SXR & ME-HXR) imaging diagnostics have been designed built and installed by an international collaboration in WEST (W Environment in Steady-state Tokamak), at the CEA site in Cadarache, France. Long pulse operation is uniquely available at the WEST tokamak with dominant electron heating without external momentum torque source and up to 16 MW of RF power for up to 1000 s. The pin-hole cameras employ a pixelated 2D x-ray detector in which the lower energy threshold for photon detection can be adjusted independently on each pixel of the detector. These versatile Si and CdTe multi-energy systems provide unprecedented improvement in throughput and signal-to-noise-ratio enabling adequate spatial and time-resolution ($\Delta r/a \sim 2\%$, $\Delta t \sim 1$ ms) as well as energy discrimination at complementary ranges of $E_{photon} \sim 1\text{-}10 \times T_{e,0}$ and $E_{photon} \sim 10\text{-}100 \times T_{e,0}$ for the SXR and HXR options, respectively. This remarkable flexibility is assisting the diagnostics of the core electron temperature and tungsten impurity density profiles, as well as enabling studies of the plasma startup, electron-thermal transport and tungsten accumulation, as well as the identification and effects of W-UFOs, loss of fast electrons in the W ITER-like divertor, among many others.

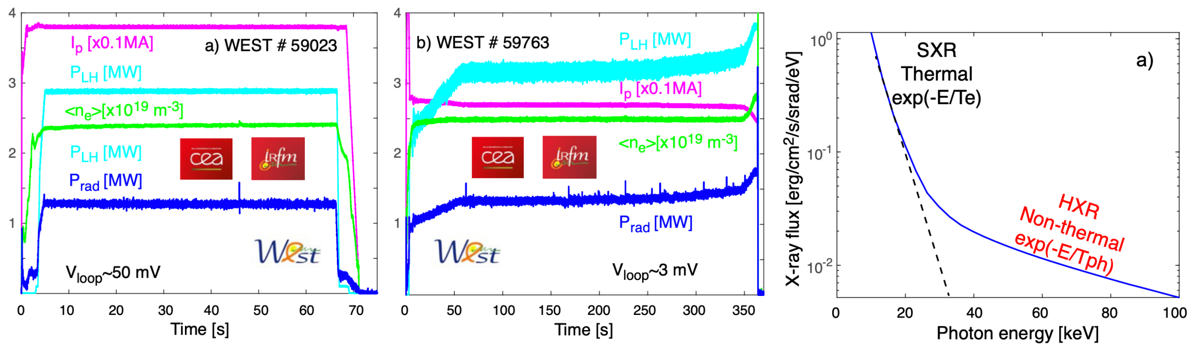

FIG. 1. (Color online) Overview discharge traces for typical 60-70 s shots as well as record 364 s plasma with a pulse duration up to $\sim 6000 \times \tau_E$. Tungsten UFO's were observed in both discharges as shown in the transients of P_{rad}. Typical x-ray Bremsstrahlung photon fluxes from LHCD plasma's Maxwellian and non-Maxwellian components are shown in c)

2. MOTIVATION FOR THE USE OF NEW ADAPTIVE TECHNOLOGY

Long pulse operation can be achieved at WEST (see Fig. 1) at a nominal magnetic field of 3.7 T with dominant electron heating and no external momentum source up to 16 MW of RF power for 1000 s (7 MW of LHCD and 9 MW ICRH). An additional 1 and 3 MW of electron cyclotron heating will be installed in the Fall of 2025. An example of the x-ray energy flux emitted from typical LHCD distributions is shown in Fig. 1-c), where the spectra follow the typical thermal dependency ($\exp(-E/T_e)$) at low-energies, with a different $\exp(-E/T_{ph})$ dependency at high-energies where T_{ph} is the typical LHCD photon-temperatures of approximately 60 keV. The Bremsstrahlung emission at low photon energies is of the order of 100× stronger than at high energies. However, a slightly more realistic estimate can reach up to $\times 10^3$ since radiation is dominated mainly by line-emission and radiative recombination instead of that of the ideal Bremsstrahlung (not shown here). To access new physics and operational expertise in a tungsten environment, two versatile multi-energy soft and hard x-ray cameras have been developed, calibrated, and deployed at WEST, providing new measurements of the local x-ray emissivity in multiple energy ranges simultaneously. The thermal SXR emission is probed with a Si-detector, while the HXR sensor uses CdTe.

Configuration	Si-detector: Thermal plasmas	CdTe-detector: Non-thermal plasmas
Low threshold-energy:	• Spectra dominated by tungsten line-emission ($2<E_{ph}<10$ keV) $\Rightarrow$ n_W, C_W, δZ_{eff} • *Physics studies*: - Impurity transport (w/o LHCD, ECRH and/or ICRH) $\Rightarrow$ n_W, D_W and V_W - Impurity density asymmetries (e.g. electron vs ion-heating) - Plasma startup (focused on n_W) - Identification and impact of W-UFOs	• Spectra dominated by continuum-emission ($10<E_{ph}<20$ keV) $\Rightarrow$ T_e, Z_{eff} • *Physics studies*: - LHCD Landau damping at (3-5)$\times V_{the,e}$ - LH and EC heating vs current drive - Plasma centroid and Shafranov-shift (e.g. equilibria).
High threshold energy:	• Spectra dominated by continuum-emission ($10<E_{ph}<20$ keV) $\Rightarrow$ T_e, Z_{eff} • *Physics studies*: - Electron thermal transport - Plasma startup (focused on slide-aways) - Formation of runaway beams - Plasma centroid and Shafranov-shift	• Spectra dominated by continuum-emission ($20<E_{ph}<200$ keV) $\Rightarrow$ T_{ph}, Z_{eff} • *Physics studies*: - Impact of UFOs (on LH plasma current) - Fast-e losses to W-divertor - Plasma startup - Runaway electron beams

TABLE. 1. Different applications of the multi-energy configuration using x-ray cameras fielded with Si and CdTe sensors

3. FIRST RESULTS.

This novel technology is currently being used in a variety of diagnostic-development efforts and physics studies (as shown in Table 1) with the aim of providing also real-time solutions for plasma monitoring. Examples of the first line-integrated x-ray brightness profiles from the thermal emission in multiple energy ranges with characteristic thresholds between 11 and 18 keV are shown in Figs. 2-a) and -b), using an integration time of 0.1 s for shot 59023 (10 Hz) and 1 s for 59764 (1 Hz); the spatial resolution is of the order of 2 cm. This detector has demonstrated an unprecedented flexibility in the configuration of an imaging x-ray detection system having a dynamic range spanning four to five orders of magnitude.

In this contribution we will discuss also the design and architecture of the ME-SXR and -HXR diagnostics, the various applications considered, physics measurements, as well as lessons learnt during integration to the WEST tokamak and the engineering challenges that the short (up to 30 s) and long pulse scenarios (up to 1000 s) poses to vacuum interface and electronics.

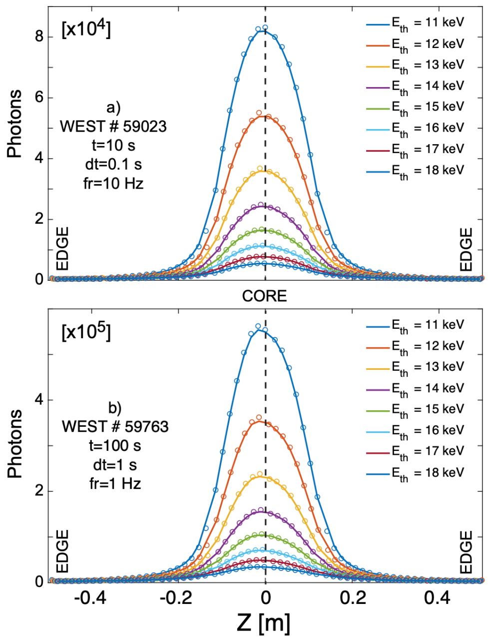

FIG. 2. X-ray line-integrated brightness profiles obtained simultaneously for eight-energy ranges for 59023 (10 Hz) and 1 s for 59764 (1 Hz) at WEST.

ACKNOWLEDGEMENTS

This work is supported by the U.S. DOE-OFES under contract number DE-AC02-09CH11466 using LFDA's 2015 DOE Early Career Award, a 2018 diagnostic development grant and a new 2021 Long-Pulse Tokamak Research Program.